

# Correlative exploration of structural, optical and electric properties of colossal dielectric Ni doped sm orthoferrites

Sajad Ahmad Mir<sup>1\*</sup>, M. Ikram<sup>2\*</sup>, K. Sultan<sup>1</sup>, Z. Habib<sup>1</sup>, H. Kausar<sup>1</sup>, K. Asokan<sup>2</sup>

<sup>1</sup>Department of Physics, National Institute of Technology, Srinagar, J&K 190006, India

<sup>2</sup>Materials Science Division, Inter University Accelerator Centre, New Delhi 110067, India

\*Corresponding author. Tel: (+91) 0194-2422032; E-mail: sajadphysics@gmail.com (S. A. Mir), ikram@nitsri.net (M. Ikram)

Received: 30 July 2015, Revised: 26 October 2015 and Accepted: 09 November 2015

## ABSTRACT

Structural, optical and dielectric properties of polycrystalline  $\text{SmFe}_{1-x}\text{Ni}_x\text{O}_3$  ( $x=0.0, 0.3$  and  $0.5$ ) samples prepared by ceramic method is presented. Lattice parameters, unit cell volume and porosity were calculated and found decreasing with an increase in Ni concentration. SEM shows an increase in grain size ( $0.2 \mu\text{m}$  to  $0.3 \mu\text{m}$ ) with an increase in Ni doping. The influences of Ni doping on optical energy band gap are investigated in the wavelength range of 200-800 nm. Dielectric properties (dielectric constant and loss) for  $\text{SmFe}_{1-x}\text{Ni}_x\text{O}_3$  were studied in the temperature range 100-400K and in the frequency range 20 kHz-1MHz. AC conductivity of pristine sample is found to be less than Ni doped samples. Various possibilities were explored to explain the observed dielectric and electric behavior of Ni doped  $\text{SmFeO}_3$  ceramics. Copyright © 2015 VBRI Press.

**Keywords:** Ferrites; morphology; dielectric properties; activation energy.

## Introduction

The  $\text{ABO}_3$  type perovskite exhibits various interesting properties such as high  $T_c$  superconductivity, colossal magneto-resistance, charge/orbital ordering, and metal-insulator transition [1-3] etc. Rare-earth ferrites exhibits strong structural, optical and electrical property, therefore, these have attracted much attention in material science research for last two decades. In addition, there has been considerable interest in rare-earth ferrites due to their low conductivity and sufficiently low losses over a wide range of frequencies, making them very good dielectric materials. The interrelationship among different properties of ferrites is governed by the method of preparation, type and amount of substitution, the oxidation states and location of the cations at the tetrahedral (A) and octahedral (B) sites in the perovskite lattice. These compounds have a variety of electronic applications [4-6] such as dynamic random access memory (DRAM), anti-corrosive protective layer coatings and gas sensors, amongst others [7-10].

Rare-earth iron oxide perovskites ( $\text{RFeO}_3$ , where R= rare earth) possesses distorted orthorhombic perovskite structure where  $\text{FeO}_6$  tilt and rotate to fill the empty space left around the R ions [11, 12]. The degree of distortion, as measured by the Fe-O-Fe bond angle, affects the structural, optical, dielectric and other properties of the compound.  $\text{RFeO}_3$  have attracted much attention due to their potential applications, such as light modulators and resonance based devices [13, 14]. Rare-earth nickel oxide perovskites ( $\text{RNiO}_3$ ) also possess an orthorhombically-distorted

perovskite structure and exhibit a clear relationship between their structural and other physical properties [15].  $\text{SmFeO}_3$  (SFO) and  $\text{SmNiO}_3$  (SNO) perovskites were investigated by many researchers with various other rare earth orthoferrites like  $\text{Gd}_x\text{Sm}_{1-x}\text{FeO}_3$  and  $\text{Er}_x\text{Sm}_{1-x}\text{FeO}_3$  [16]. Also in previous communication from this group, investigations were carried out to study many physical properties of SFNO type orthoferrite [12, 17-19].  $\text{La}_{0.8}\text{Pb}_{0.2}\text{Fe}_{1-x}\text{Ni}_x\text{O}_3$  system has been studied by song *et al.* [20] and has confirmed that partial Ni substitution at Fe-site not only increases the sensing response but also the conductivity at low dopant concentration. Blasco *et al.* studied structural and electrical properties of  $\text{Nd}_{1-x}\text{La}_x\text{NiO}_3$  and confirmed that both the properties are interdependent on each other. At room temperature SFO is insulator whereas SNO is metal. Also at ambient conditions SFO in bulk form is stable with Fe in its 3+ oxidation state while SNO in bulk form is unstable due to the necessity of an important oxygen pressure to stabilize it in its 3+ oxidation state [21]. Therefore, merging of metallic SNO in insulating SFO through the replacement of trivalent Fe with homovalent Ni in SFO may develop a system of  $\text{SmFe}_{1-x}\text{Ni}_x\text{O}_3$  (SFNO) which will be fascinating to study with regard to varied physical properties and their interplay. Several researchers thoroughly studied the transport properties of different ferrites because of their great importance in electronic applications [22-24]. But, to the best of our knowledge less attention has been paid to explore this field to study the optical, electrical and dielectric properties of SFO (where Fe is replaced by Ni) in

concert. These things motivate us to study different physical properties of SFNO for betterment of modern electronics and try to accentuate their interdependence. So, in this communication an attempt is made to study various functional properties of Ni doped SFO by distinctive characterizations viz XRD, SEM, UV-visible and dielectric spectroscopy and bring to light their correlation.

## Experimental

$\text{SmFe}_{1-x}\text{Ni}_x\text{O}_3$ , ( $0 \leq x \leq 0.5$ ) (hereafter referred SFNO) polycrystalline bulk samples were synthesized by solid state reaction method using proper stoichiometric amounts of high purity  $\text{Sm}_2\text{O}_3$ ,  $\text{Fe}_2\text{O}_3$  and  $\text{NiO}$  [25]. All these chemicals were mixed and ground into fine powder. The mixtures were pressed into pellets under hydraulic pressure. The pellets were calcinated at  $1000^\circ\text{C}$  in air for 10 h and sintered at  $1250^\circ\text{C}$  and  $1300^\circ\text{C}$  for 24 h each with intermediate grinding and pelletizations. During sintering rate of heating and cooling were kept  $3^\circ\text{C}/\text{minute}$ . The XRD studies were carried out by Bruker D8 X-ray diffractometer with  $\text{Cu K}\alpha$  radiation ( $1.5408 \text{ \AA}$ ) in  $2\theta$  range of  $20^\circ$ - $80^\circ$ . Scanning electron microscopic images were obtained using a JEOL JSM-6490LV microscope at 25 kV after covered with a thin silver layer ( $\sim 10 \text{ nm}$ ). SEM micrographs were taken at different magnifications to determine the effect of Ni substitution on the lattice and porosity of samples. UV-visible absorption spectroscopy has been performed by Hitachi U-3300 spectrophotometer in the wave length range of 200-800 nm. For dielectric measurements bulk samples of pristine and Ni doped SFO pellets were coated with thin gold coatings on both flat circular faces such that pellet acts as dielectric medium and gold coatings as electrodes of circular parallel plate capacitor and then dielectric measurements were performed with Agilent LCR meter and LakeShore 325 temperature controller. The dielectric constant,  $\epsilon'$  and the loss tangent,  $\tan\delta$  were calculated from measured capacitance values as a function of frequency in the range of 20 kHz-1MHz, composition and temperature in the range of 100 K-400 K.  $\epsilon'$  was calculated using formula  $\epsilon' = Cd/\epsilon_0 A$ , where  $C$  is the capacitance,  $d$  the thickness of the sample,  $\epsilon_0$  the permittivity of free space and  $A$  the cross-section area. The ac electrical conductivity,  $\sigma_{ac}$  was calculated from the data of  $\epsilon'$  and  $\tan \delta$  using the relation  $\sigma_{ac} = 2\pi f \epsilon_0 \epsilon' \tan \delta$ , where  $f$  is the ac frequency.

## Results and discussion

### Structural, morphological and optical investigation

The X-ray diffraction pattern of SFNO compounds is shown in **Fig. 1** and peaks indexed by using Powder X [26] confirm the orthorhombic crystal structure. Variations in peak intensities in XRD pattern were noticed under the effect of Ni substitution. Peak shift towards higher  $\theta$  value were also noticed as shown in inset of **Fig. 1**. From XRD data, lattice parameters and unit cell volume were calculated and tabulated in **Table 1**. It was observed that an increase in Ni substitution results in decrease of unit cell volume. This is because  $\text{Ni}^{3+}$  ion has smaller ionic radius than  $\text{Fe}^{3+}$  ions as previously reported by our group [27]. However, the results of this study show a very slight

variation in lattice parameters of SFNO. This may be due to different sintering environment used while the synthesis of SFNO samples. So, it can be suggested that in SFNO samples a decrease in the values of lattice constants is due to a larger fraction of  $\text{Fe}^{3+}$  ( $0.785 \text{ \AA}$ ) ions of larger ionic radii are replaced by smaller  $\text{Ni}^{3+}$  ( $0.70 \text{ \AA}$ ) ions.

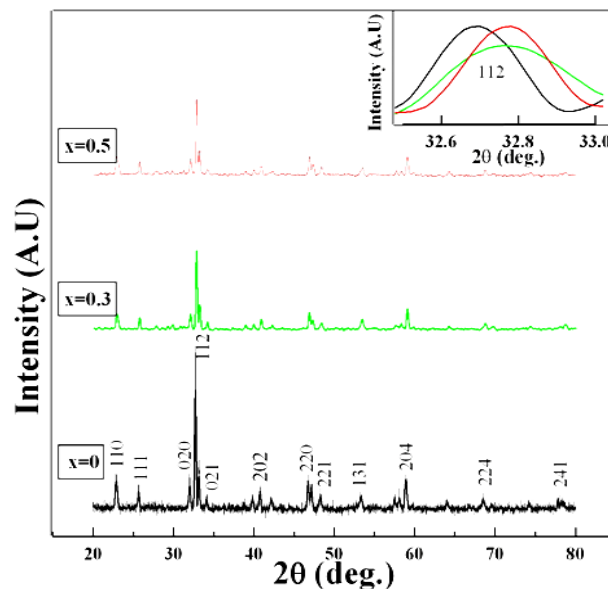


**Fig. 1.** X-ray diffraction pattern of  $\text{SmFe}_{1-x}\text{Ni}_x\text{O}_3$  samples with inset at right top to depict the shift in [112] peak with Ni concentration.

**Table 1.** Lattice parameters and unit cell volume of  $\text{SmFe}_{1-x}\text{Ni}_x\text{O}_3$  for  $x=0.0, 0.3$ , and  $0.5$ .

Composition	a (Å)	b (Å)	c (Å)	V (Å <sup>3</sup> )
X=0.0	5.394	5.589	7.711	232.464
X=0.3	5.387	5.580	7.671	230.586
X=0.5	5.384	5.575	7.671	230.251

The average particle size was determined using Scherrer formula [28] and found to increase with an increase in Ni substitution. The bulk density,  $d_b$  in  $\text{g}/\text{cm}^3$  is determined using the relation  $d_b = m/(r^2h)$ , where  $m$ ,  $r$  and  $h$  are the mass, radius and height respectively of the sample. The X-ray density in  $\text{g}/\text{cm}^3$  of all synthesized samples was calculated using the relation  $d_x = 8M/Na^3$ , Where  $M$  is molecular weight,  $N$  is Avogadro's number and  $a$  the lattice parameter. An increase in Ni content is noticed to reduce densification in the SFO. The porosity of samples was devised from the formula  $P = (1 - d_b / d_x)$ . The porosity values of SFNO samples are listed in **Table 2**.

**Table 2.** Sample mass, Bulk density, X-ray density and porosity of  $\text{SmFe}_{1-x}\text{Ni}_x\text{O}_3$  for  $x=0.0, 0.3$ , and  $0.5$ .

Composition	Sample mass $m$ (g)	Bulk density $d_b$ ( $\text{g}/\text{cm}^3$ )	X-ray density $d_x$ ( $\text{g}/\text{cm}^3$ )	Porosity $P$ (%)
X=0.0	0.155	20.495	21.698	5.544
X=0.3	0.165	19.834	21.713	8.654
X=0.5	0.220	19.393	21.516	9.867

**Fig. 2** shows the porosity versus composition of SFNO samples. It was also found that porosity increases with an increase in Ni composition.

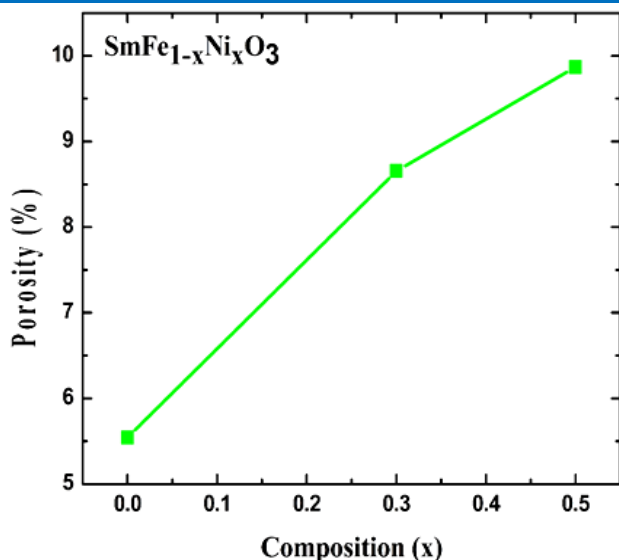


**Fig. 2.** Variation of Porosity with Ni composition for  $\text{SmFe}_{1-x}\text{Ni}_x\text{O}_3$  ferrite.

The SEM images of SFNO pellets with their magnified images (A, B and C) and EDX spectra (A', B' and C') are shown in **Fig. 3**. The microstructure reveals the well sintered nature of the pellets. The crystallinity in SFNO type system becomes more complicated with incorporation of Ni as proposed by various authors in different transition metal oxide families [29-31].

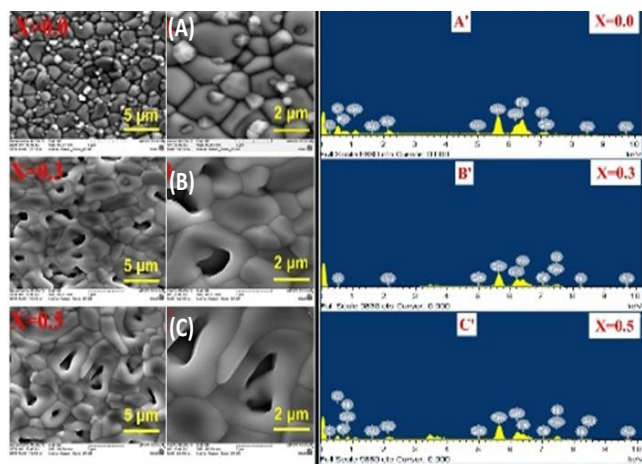


**Fig. 3.** SEM Photomicrographs illustrating the porosity and surface order with increasing Ni substitution for SFNO at  $x=0.0, 0.3$  and  $0.5$ . (A), (B) and (C) represent SEM Photomicrographs at higher magnification. (A'), (B') and (C') represent EDX pattern of above morphology.

However, these images show the increase in grain size with an increase in Ni concentration. The average grain size is  $0.2 \mu\text{m}$ ,  $2 \mu\text{m}$  and  $3 \mu\text{m}$  for pristine, SFNO ( $x=0.3$ ) and SFNO( $x=0.5$ ) respectively. The densification reduces due to the impregnation of Ni dopant concentration making the morphology of SFNO samples more porous and slacked. These morphological consequences are consistent with the results acquired from XRD investigation. This outcome may be a reason for colossal dielectric constant of SFNO ceramics discussed in the next subsection of this paper. The presence of all elements corresponding to pristine sample, SFNO ( $x=0.0$ ) shows Sm, Fe and O and to Ni doped

samples, SFNO ( $x=0.3, 0.5$ ) shows Sm, Fe, Ni and O are confirmed from EDX pattern as shown in **Fig. 3** (A', B' and C').

From UV-visible spectroscopy of SFNO it was observed that maximum absorption which depends on type of material takes place in lower wavelength range (around  $200 \text{ nm}$  wavelength for SFNO) suggests that the optical energy gap between occupied states of valence band to unoccupied states in conduction band is of higher order [32]. UV-visible spectroscopy of SFNO systems also reveals that the maximum absorption peak is found to exhibit red shift as we move from lower Ni doping level to higher Ni doping level. Contraction in unit cell volume, and lattice of crystal and its impact on the crystal field potential of the system after Ni substitution may be the reason behind such shift in maximum absorption peak. This outcome of UV-visible spectroscopy is in good accord with XRD data. **Fig. 4** shows the variation of  $(\text{abs.}E)^{1/2}$  with  $E(\text{eV})$ . The values of optical energy band gap,  $E_g$ , for SFNO samples are calculated by extended linear region of the curves in the graph to meet the  $E(\text{eV})$  axis when  $(\text{Abs.}E)^{1/2}$  becomes equal to zero.

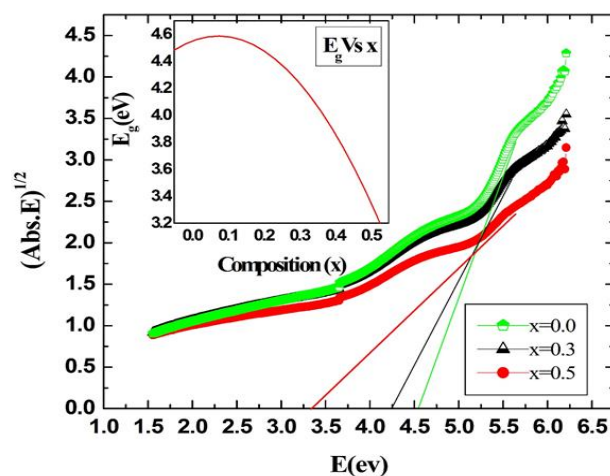


**Fig. 4.** UV-Visible spectrograph of  $(\text{Abs.}E)^{1/2}$  Versus  $E(\text{eV})$  for  $x=0.0, 0.3, 0.5$ . The inset of the graph shows Optical energy band gap versus Ni composition in  $\text{SmFe}_{1-x}\text{Ni}_x\text{O}_3$  ( $0 \leq x \leq 0.5$ ).

**Table 3.** Room temperature values of tangent loss, dielectric constant, AC conductivity and optical band gap for  $\text{SmFe}_{1-x}\text{Ni}_x\text{O}_3$  for  $x=0.0, 0.3$ , and  $0.5$ .

Composition	Tangent Loss $\tan\delta$ (1MHz)	Dielectric Constant $\epsilon'$ (1MHz)	AC Conductivity $\sigma_{ac}$ ( $\Omega^{-1}\text{cm}^{-1}$ ) (1MHz)	Optical Band Gap $E_g$ (eV)
X=0.0	0.164	1205	0.001	4.549
X=0.3	2.644	15639	0.263	4.240
X=0.5	2.705	17940	0.279	3.356

The maximum  $E_g$  value of  $4.549 \text{ eV}$  is for pristine SFNO sample and for comparison the calculated  $E_g$  values for  $x=0.3$  and  $x=0.5$  composition of the SFNO sample are tabulated in **Table 3**.

The calculated optical energy band gap values show that Optical energy gap between O  $2p$  and Fe  $3d/\text{Ni } 3d$  goes on decreasing with Ni substitution in SFNO system. Inset of **Fig. 4** shows the decreasing trend of optical energy band gap with an increase in Ni composition in SFNO system.

## Dielectric studies

**Fig. 5(a)** displays the variation of dielectric loss tangent,  $\tan\delta$ , as a function of frequency at different temperatures for various Ni concentrations. It demonstrates that  $\tan\delta$  increases with Ni substitution in SFNO samples at fixed frequency and temperature. Maximum  $\tan\delta$  (2.705) is observed for  $x=0.5$  composition at a frequency of 1MHz at temperature of 300K. The value of  $\tan\delta$  is maximum for all SFNO samples at lower frequency of 20 kHz. At lower frequency the jumping frequencies of localized charge carriers are almost equal to that of applied ac electric field. Furthermore, the decrease in  $\tan\delta$  with increase in frequency is in accordance with Koops phenomenological model. The  $\tan\delta$  is considered to be the most important part of the total core loss in ferrites [33, 34].

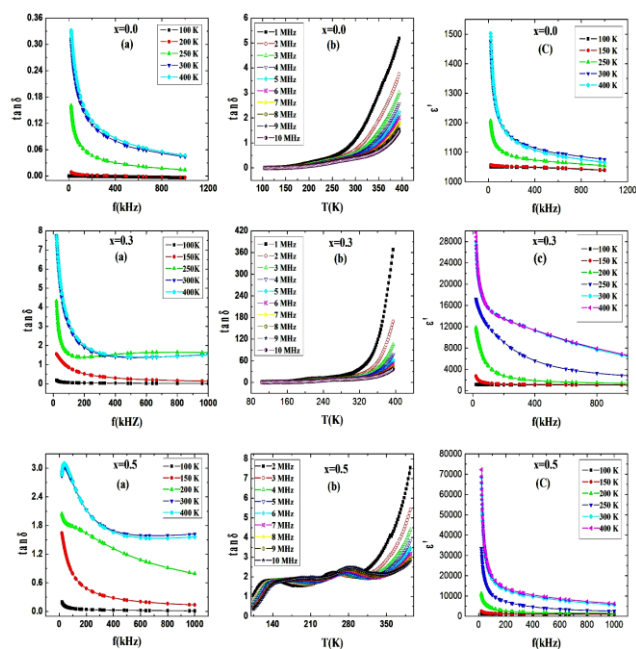


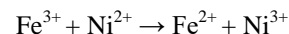
**Fig. 5.** (a) Tangent Loss versus frequency at different temperatures, (b) Tangent Loss versus temperature at different frequencies, and (c) Dielectric Constant versus frequency at different temperatures for  $\text{SmFe}_{1-x}\text{Ni}_x\text{O}_3$  at  $x=0.0, 0.3$  and  $0.5$ .

**Fig. 5(a)** also shows an increase in  $\tan\delta$  with temperature. Such an increase in  $\tan\delta$ , is because of the fact that at high temperature, high energy may be able to activate more electron exchange between  $\text{Fe}^{3+} \rightarrow \text{Fe}^{2+}$  through high resistive grain boundary gives local displacement of electrons in the direction of applied field which leads to incomplete polarization and thus an increase in tangent loss.

**Fig. 5(b)** shows the variation of dielectric loss tangent with temperature at different Ni compositions. It seems that  $\tan\delta$  has, in general, small values and indicates a maximum around 400 K. The appearance of a maximum in  $\tan\delta$  could be explained according to Koop's model in which the solid is assumed to be composed of grains and grain boundaries. Each one has different parameters where the grains have low resistivity and large thickness. Moreover, it was assumed that each of the grains and grain boundaries has its characteristic peak [35]. A small peak is observed at low temperature around 150 K in  $\tan\delta$  versus temperature plot in case of SFNO ( $x=0.5$ ) for all frequencies which may

be attributed to the existence of one thermally activated relaxation in case of SFNO ( $x=0.5$ ). The peak position shifted towards higher values of temperature as the measuring frequency increases. Another peak is observed in the same plot in case of SFNO ( $x=0.5$ ) around 260 K for all frequencies. This indicates that there may be the existence of another thermally activated relaxation. In case of SFNO ( $x=0.3$ ) the thermally activated relaxation phenomenon occur around 220 K. **Fig. 5(b)** also shows that  $\tan\delta$  as a function of temperature is maximum for SFNO ( $x=0.3$ ) than pristine. At a frequency of 1MHz and temperature of 300 K  $\tan\delta$  is 26.6 for Ni doped SFNO ( $x=0.3$ ) and 1.2 for pristine SFO. This indicates that the presence of Ni which prefers Fe-site in SFO and strengthens the dipole dipole interaction leading to hindrance to the rotation of dipoles and hence increase in  $\tan\delta$  [36]. But that  $\tan\delta$  values with respect to temperature for SFNO ( $x=0.5$ ) are less than SFNO ( $x=0.3$ ). This may be due to saturation limit of Ni substitution. At high temperatures the observed maximum in  $\tan\delta$  may be due to charge exchange between  $\text{Fe}^{2+} \rightarrow \text{Fe}^{3+}$  through high resistive grain boundary which results in incomplete polarization and maximum in tangent loss for all samples.

**Fig. 5(c)** for different Ni compositions displays variation of dielectric constant,  $\epsilon'$ , as a function of frequency at different temperatures from 20 kHz-1 MHz for SFNO. It is evident that for a particular concentration,  $\epsilon'$  decreases with increase in frequency which is reported for some other ferrites [37]. It is also clear that Ni substituted SFNO samples possess dielectric constant of the order of  $10^3$ - $10^4$ . Colossal dielectric constant has been also observed for different ceramics synthesized by solid state reaction method [38]. The increase in the  $\epsilon'$  with Ni ions substitution in the SFNO samples can be explained on the basis of Maxwell-Wagner type of polarization. The whole polarization in ferrites is mainly contributed by space charge polarization and hopping exchange. Space charge polarization is a result of the presence of higher conductivity phases (grains) in the insulating matrix (grain boundaries) of dielectrics, causing localized accumulation of charge under the influence of an electric field. Hopping exchange is a result of the charges exchange between two localized states governed by density of the localized state and resultant displacement of charges with respect to the external field. The addition of Ni ions in the SFNO samples increases the  $\text{Fe}^{2+}$  ions on B-sites which are mainly responsible for both space charge polarization and hopping exchange between the localized states. On substituting Ni at Fe-site of SFO following reaction takes place to increase  $\text{Fe}^{2+}$  ions and maintain charge balance:



Electronic hopping between  $\text{Fe}^{2+} \rightarrow \text{Fe}^{3+}$  and  $\text{Ni}^{2+} \rightarrow \text{Ni}^{3+}$  and the presence of ferrous ions in large number is the reason for higher  $\epsilon'$ . Therefore, increasing of Ni ions content causes an increase in the polarization which is accompanied by an increase of  $\epsilon'$  of the SFNO composition. Increase in grain size and porosity with Ni doping can be another possible reason for colossal  $\epsilon'$  of SFNO systems. Higher value of  $\epsilon'$  in SFNO is observed for the  $x=0.5$  composition at frequency of 1MHz and

temperature 300 K. For comparison room temperature  $\mathcal{E}'$  at 1MHz of pristine and SFNO ( $x=0.3$  and  $0.5$ ) samples are shown in **Table 2**. **Fig. 5(c)** shows that the maximum values of  $\mathcal{E}'$  are obtained for all pristine and Ni doped samples at lower frequency around 20kHz. Koops proposed that the effect of grain boundaries is predominant at lower frequencies [39]. The thinner the grain boundary, the higher the  $\mathcal{E}'$  is. However, the  $\mathcal{E}'$  decreases with increasing frequency till it attains constant value which is attributed to the fact that after a certain frequency limit the charge exchange between  $\text{Fe}^{2+}$  and  $\text{Fe}^{3+}$  cannot follow the alternating nature of field [40].

**Fig. 5(c)** also shows an increase in  $\mathcal{E}'$  with temperature, which suggests the presence of more  $\text{Fe}^{2+}$  ions in the conventionally prepared ferrites, rendering the ortho ferrite structure highly heterogeneous. Since  $\text{Fe}^{2+}$  ions are more easily polarizable, the larger the number of  $\text{Fe}^{2+}$  ions, the higher would be the  $\mathcal{E}'$  [41-44].

From the results of dielectric constant, grain size and porosity of SFNO system it has been observed that these three properties are correlated with each other. Higher porosity and large grain size results in abnormal high dielectric constant of SFNO materials which may help in miniaturization of capacitive electronic elements for the further development of modern electronic industry.

#### A.C conductivities of SFNO

The theoretical study shows that dielectric constant and dielectric loss are inversely proportional to frequency while the ac electrical conductivity is directly proportional to frequency [45-47]. Similar relationship is observed between  $\sigma_{ac}$  and frequency for SFNO samples. The dependence of  $\sigma_{ac}$  on temperature at frequencies ranging from 1MHz to 10MHz is observed at different Ni compositions. The graph (not shown here) between  $\ln\sigma_{ac}$  and  $T/1000$  K shows that at 1MHz the value of  $\ln\sigma_{ac}$  increases from  $-19.20$  to  $-10.27$   $\Omega^{-1}\text{cm}^{-1}$ ,  $-12.64$  to  $-4.74$   $\Omega^{-1}\text{cm}^{-1}$  and  $-12.66$  to  $-3.94$   $\Omega^{-1}\text{cm}^{-1}$  for SFNO sample at  $x=0.0$ ,  $x=0.3$  and  $x=0.5$  respectively in the temperature range of  $1 \times 10^{-1}\text{K}$  to  $4 \times 10^{-3}\text{K}$ . Akin variations were also observed at other higher frequencies of 2MHz, 3MHz, 4MHz, 5MHz, 6MHz, 7MHz, 8MHz, 9MHz and 10MHz. So, the conductivity increases with an increase in temperature and thus, obeys semiconductor behavior. Similar behavior was confirmed by Bandi Vittal Prasad et al in  $\text{SmFeO}_3$  system [48].

The activation energy,  $E_a$ , at various frequencies of 2 MHz, 3 MHz, 4 MHz, 5 MHz, 6 MHz, 7 MHz, 8 MHz, 9 MHz and 10 MHz was calculated from the slope of graph between  $\ln\sigma_{ac}$  versus inverse of temperature shown in **Fig. 6**, using the Arrhenius relation  $\sigma_{ac} = \sigma_0 \exp(-E_a/KT)$  for different compositions of Ni, where,  $\sigma_{ac}$  is ac electrical conductivity at absolute temperature,  $T$ ,  $\sigma_0$  stands for the pre-exponential term and  $K$  the Boltzmann constant. Although the activation energy stays almost fixed for all compositions of SFNO but conductivity enhances with an increase in Ni doping [49]. It is because Ni substitution in the SFO leads to carrier doping which results in decrease in the energy gap and hence increases the conductivity of the sample and the same has been reported here [50] for La ferrites.

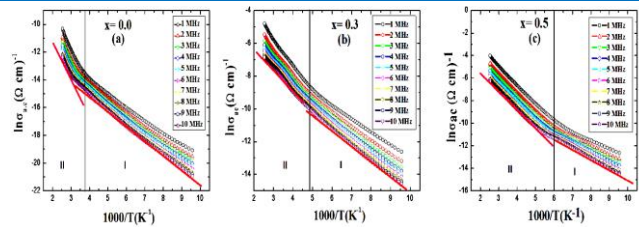


**Fig. 6.** AC conductivity versus inverse of temperature at different frequencies, for  $\text{SmFe}_{1-x}\text{Ni}_x\text{O}_3$  at  $x=0.0, 0.3$  and  $0.5$ .

**Fig. 6(a-c)** represents ac conductivity versus temperature in the temperature range 80-380 K of SFO and SFNO ceramics at various frequencies (1-10 MHz). The behavior of ac conductivity as a function of the temperature at different frequencies of SFNO ( $x=0.0, 0.3$  and  $0.5$ ) samples is similar in nature. This an indication that  $\sigma_{ac}$  obeys Jonscher's power law which is a typical for hopping conduction. Interestingly two different regimes can be distinguished clearly as shown in the **Fig. 6**. The boundary of two regions lies around 270K, 208K and 166K for SFO, SFNO( $x=0.3$ ) and SFNO ( $x=0.5$ ) samples respectively. So, there will be two values of activation energy of ac conduction for two different regions and may be distinctive mechanisms responsible for ac conduction. The absolute values of  $E_a$  in the region I are 0.99 eV, 0.10 and 0.12 eV and in the region II are 0.65 eV, 0.30 eV and 0.23 eV for SFO, SFNO( $x=0.3$ ) and SFNO ( $x=0.5$ ) samples respectively. In perovskites, the value of  $E_a$  in the range of 0.6-1.2 eV that suggests the mechanism of the conduction is due to the motion of electrons from the second ionization of oxygen vacancies. It is only in pristine sample (SFO) above 270K the  $E_a > 0.6$  eV. At lower temperatures, the mobility of oxygen vacancies is low; however, with an increase in temperature oxygen vacancies are activated and contribute widely to the electrical mechanism of SFO ceramics. In the case of  $E_a < 0.4$  eV the conduction mechanism is considered charge (electron and hole) hopping [51]. For Ni doped samples (SFNO) we observe  $E_a < 0.4$  eV over the whole observed temperature range and expect this mechanism to apply here as well.  $E_a$  calculated from conductivity are consistent with  $\text{Fe}^{2+}\text{Fe}^{3+}/\text{Ni}^{2+}-\text{Ni}^{3+}$  electron/hole hopping (small polaron) as the dominant conduction mechanism at all temperatures of Ni doped samples; however ionic conduction for SFO sample at high temperatures.

From the results of UV-visible spectroscopy and electric measurements it can be conferred that the optical energy band gap and ac conductivity of SFNO systems are correlated with each other. In SFNO compositions lower optical energy band gap results in higher ac conductivity.

#### Conclusion

$\text{SmFe}_{1-x}\text{Ni}_x\text{O}_3$  polycrystalline ferrites were prepared by ceramic method. A correlation is found between Ni doping caused porosity, grain size and dielectric behavior of SFNO ferrite. From the results of present study porosity and grain size escalation of  $\text{SmFe}_{1-x}\text{Ni}_x\text{O}_3$  materials with an increase in Ni doping leads to a colossal dielectric constant ( $\sim 10^4$ ) which is a staple condition for any material to be used in

storage based devices in the microelectronic industry. Small polaron hopping is found to be the dominant mechanism contributes to the electrical behavior of SFNO ceramics. Present study highlights the semiconductor-like behavior of  $\text{SmFe}_{1-x}\text{Ni}_x\text{O}_3$  system. It also reports, interdependence between optical energy band gap and ac conductivity in Ni doped Sm orthoferrites. Finally the enhancement of Ni content at the Fe site of investigated ceramics leads to increase the ac conductivity, dielectric constant, porosity, grain size and decrease the optical energy band gap. These properties of materials intern to be a potential candidate for dielectric resonator and dynamic random access memories.

#### Acknowledgements

One of the authors (SAM) would like to thank Dr. R.J. Choudhary, IUC-CSR, Indore (MP) for discussions. Authors would also like to thank Director Inter University Accelerator Center, New Delhi for providing every kind of experimental facilities and Director National Institute of Technology, Srinagar, J&K for constant encouragement.

#### Reference

- Torrance, J. B.; Lacorre, P.; Nazzal, A. I.; Ansaldo, E. J.; Niedermayer, C., *Phys. Rev. B* **1992**, *45*, 8209.  
DOI: [10.1103/PhysRevB.45.8209](https://doi.org/10.1103/PhysRevB.45.8209)
- Zhou, J. S.; Goodenough J. B.; Dabrowski, D., *Phys. Rev. Lett.* **2005**, *94*, 226602.  
DOI: [10.1103/PhysRevLett.94.226602](https://doi.org/10.1103/PhysRevLett.94.226602)
- Sultan, K.; Habib, Z.; Jan, A.; Mir, S. A.; Ikram, M.; Asokan, K., *J. Adv. Mat. Lett.* **2014**, *5*, 9.  
DOI: [10.5185/amlett.2013.6496](https://doi.org/10.5185/amlett.2013.6496)
- Sultan, K.; Ikram, M.; Asokan, K., *Vacuum* **2014**, *99*, 251.  
DOI: [10.1016/j.vacuum.2013.06.014](https://doi.org/10.1016/j.vacuum.2013.06.014)
- Abdeen, A.M., *J. Magn. Magn. Mater.* **1998**, *185*, 199.  
DOI: [10.1016/S0304-8853\(97\)01144-X](https://doi.org/10.1016/S0304-8853(97)01144-X)
- Iwanchi, K., *J. Appl. Phys.* **1971**, *10*, 1520.  
DOI: [10.1143/JJAP.10.1520](https://doi.org/10.1143/JJAP.10.1520)
- Hemberger, J.; Lunkenheimer, P.; Fichtl, R.; Krug von Nidda, H. A.; Tsurkan, V.; Loidl, A., *Nature London* **2005**, *434*, 364.  
DOI: [10.1038/nature03348](https://doi.org/10.1038/nature03348)
- Takasu, H., *J. Electroceram.* **2000**, *4*, 327.  
DOI: [10.1023/A:1009910525462](https://doi.org/10.1023/A:1009910525462)
- Scott, J.F., *Ann. Rev. Mater. Sci.* **1998**, *28*, 79.  
DOI: [10.1146/annurev.matsci.28.1.79](https://doi.org/10.1146/annurev.matsci.28.1.79)
- Kington, A.I.; Streiffer, S. K.; Basceri, C.; Summerfield, S.R., *MRS Bull.* **1996**, *21*, 46.  
DOI: [10.1557/S0883769400035910](https://doi.org/10.1557/S0883769400035910)
- Mizokawa, T.; Fujimori, A.; Arima, T.; Tokura, Y.; Mori, N.; Akimitsu, J., *Phys. Rev. B* **1995**, *52*, 13865.  
DOI: [10.1103/PhysRevB.52.13865](https://doi.org/10.1103/PhysRevB.52.13865)
- Mir, F. A.; Ikram, M.; Kumar, R., *Solid State Sciences.* **2011**, *13*, 1994.  
DOI: [10.1016/j.solidstatesciences.2011.09.001](https://doi.org/10.1016/j.solidstatesciences.2011.09.001)
- Moskvin, A.S.; Ovanesyan, N.S.; Trukhtanov, V.A., *Hyperfine Interact.* **1975**, *1*, 265.  
DOI: [10.1007/BF01022459](https://doi.org/10.1007/BF01022459)
- Vasques, C.; Kogerler, P.; Lopez-Quintela, A., *J. Mater. Res.* **1998**, *13*, 451.  
DOI: [10.1557/JMR.1998.0058](https://doi.org/10.1557/JMR.1998.0058)
- Medarde, M.L., *J. Phys. Condens. Matter.* **1997**, *9*, 1679.  
DOI: [10.1088/0953-8984/9/8/003](https://doi.org/10.1088/0953-8984/9/8/003)
- Sherwood R C, Uitert L G, Wolfe R, LeCraw R C, *phys Lett* **1967**, *25A*, 297.  
DOI: [10.1016/0375-9601\(67\)90659-7](https://doi.org/10.1016/0375-9601(67)90659-7)
- Bashir, A.; Ikram, M.; Kumar, R.; Chae, K.H.; Choi, W.K.; Reddy, V.R., *J. Phys. Condens. Matter.* **2009**, *21*, 325501.  
DOI: [10.1088/0953-8984/21/32/325501](https://doi.org/10.1088/0953-8984/21/32/325501)
- Kumar, R.; Choudhary, R.J.; Ikram, M.; Shukla, D.K.; Mollah, S.; Thakur, P.; Chae, K.H.; Angadi, B.; Choi, W.K.; *J. Appl. Phys.* **2007**, *102*, 073707.  
DOI: [10.1063/1.2786895](https://doi.org/10.1063/1.2786895)
- Sajad, A.; Mir, M.; Ikram, K.; Asokan, K. *RSC Adv.* **2015**, *5*, 85082.  
DOI: [10.1039/c5ra17045a](https://doi.org/10.1039/c5ra17045a)
- Song, P.; Qin, H.; Huang, S.; Liu, X.; Zhang, R.; Hu, J.; Jiang, M., *Mater. Sci. Eng. B* **2007**, *138*, 193.  
DOI: [10.1016/j.mseb.2006.11.022](https://doi.org/10.1016/j.mseb.2006.11.022)
- Girardot, C.; Pignard, S.; Weiss, F.; Kreisel, J., *A. Phys. Lett.* **2011**, *98*, 241903.  
DOI: [10.1063/1.3599580](https://doi.org/10.1063/1.3599580)
- Parvatheeswara Rao, B. and Rao, K.H., *J. Mater. Sci.* **1997**, *32*.  
DOI: [10.1023/A:1018683615616](https://doi.org/10.1023/A:1018683615616)
- Murthy, V.R.K.; Sobhanadri, J.; *Proc. Seminar on Elect. And Spec. Ceramic Materials, India* **1976**, 139.
- Rahman, S. A., *Egypt. J. Solids* **2006**, *29*, 131.
- Mir, S. A.; Ikram, M.; Asokan, K.; *Optik* **2014**, *125*, 6903.  
DOI: [10.1016/j.ijleo.2014.08.050](https://doi.org/10.1016/j.ijleo.2014.08.050)
- Carvajal, J. R., *Physica B.* **2002**, *192*, 55.  
DOI: [10.1016/0921-4526\(93\)90108-i](https://doi.org/10.1016/0921-4526(93)90108-i)
- Bashir, A.; Ikram, M.; Kumar, R.; Lisboa Filho, P. N. and Thakur, P., *Mater. Sci. Eng., B* **2010**, *172*, 242.  
DOI: [10.1016/j.mseb.2010.05.024](https://doi.org/10.1016/j.mseb.2010.05.024)
- Klug, H.P.; Alexander, L. E., *X-ray Diffraction Procedure, second ed, Wiley, New York* **1974**.
- Chyuan, I.; Fu, S.L., *J. Mater. Sci.* **1990**, *25*, 4699.  
DOI: [10.1007/BF01129927](https://doi.org/10.1007/BF01129927)
- Zhai, J.; Yao, X.; Shen, J.; Zhang, L.; Chen, H., *J. Phys. D* **2004**, *37*, 748.  
DOI: [10.1088/0022-3727/37/5/016](https://doi.org/10.1088/0022-3727/37/5/016)
- Kumara, M.; Gargb, A.; Kumar, R. and Bhatnagar, M.C., *Physica B* **2008**, *403*, 1819.  
DOI: [10.1016/j.physb.2007.10.144](https://doi.org/10.1016/j.physb.2007.10.144)
- Vidyasagar, C. C.; Arthoba Naik, Y.; Venkatesh, T. G.; Viswanath, R., *Powder Tech.* **2011**, *214*, 337.  
DOI: [10.1016/j.powtec.2011.08.025](https://doi.org/10.1016/j.powtec.2011.08.025)
- Brockman, F. G.; Dowling, P. H.; Steneck, W. G., *Phys. Rev.* **1949**, *75*, 1440.  
DOI: [10.1103/PhysRev.75.1440](https://doi.org/10.1103/PhysRev.75.1440)
- Mangalaraja, R. V.; Ananthakumar, S.; Manohar, P.; Gnanam, F. D., *J. Magn. Magn. Mater.* **2002**, *253*, 56.  
DOI: [10.1016/S0304-8853\(02\)00413-4](https://doi.org/10.1016/S0304-8853(02)00413-4)
- Sattar A. A. and Rahman, S. A., *Phys. Stat. Sol. (a)* **2003**, *200*, 415.  
DOI: [10.1002/pssa.200306663](https://doi.org/10.1002/pssa.200306663)
- Amarendra, K.; Goel, T. C.; Mendiratta, R. G.; Thakur, O. P.; Prakash, C., *J. Appl. Phys.* **2002**, *91*, 6626.  
DOI: [10.1063/1.1470256](https://doi.org/10.1063/1.1470256)
- Anjum, G.; Kumar, R.; Mollah, S.; Shukla, D.; Kumar S.; Lee, C.G., *J. Appl. Phys.* **2010**, *107*, 103916.  
DOI: [10.1063/1.3386527](https://doi.org/10.1063/1.3386527)
- Abdeen, A.M., *J. Magn. Magn. Mater.* **1999**, *192*, 121.  
DOI: [10.1016/S0304-8853\(98\)00324-2](https://doi.org/10.1016/S0304-8853(98)00324-2)
- Koops, C., *Phys. Rev.* **1951**, *83*, 121.  
DOI: [10.1103/PhysRev.83.121](https://doi.org/10.1103/PhysRev.83.121)
- Abo El Ata A M, Attia S M and Meaz T M, *Solid State Sci.* **2004**, *6*, 61.  
DOI: [10.1016/j.solidstatesciences.2003.10.006](https://doi.org/10.1016/j.solidstatesciences.2003.10.006)
- Kratzch, M., *Phys. Stat. Sol. (b)* **1964**, *6*, 479.  
DOI: [10.1002/pssb.19640060218](https://doi.org/10.1002/pssb.19640060218)
- Fang, P.H., *Phys. Stat. Sol. (b)* **1965**, *9*, 793.  
DOI: [10.1002/pssb.19650090316](https://doi.org/10.1002/pssb.19650090316)
- Verma, A.; Goel, T.C.; Mendiratta, R.G.; Alam, M.I., *Mater. Sci. Eng., B* **1999**, *60*, 156.  
DOI: [10.1016/S0921-5107\(99\)00019-7](https://doi.org/10.1016/S0921-5107(99)00019-7)
- Mangalaraja, R.V.; Ananthakumar, S.; Manohar, P.; Gnanam, F.D., *Materials Lett.* **2003**, *57*, 1151.  
DOI: [10.1016/S0167-577X\(02\)00947-3](https://doi.org/10.1016/S0167-577X(02)00947-3)
- Habib, Z.; Majid, K.; Ikram, M.; Asokan, K., *J. Electron. Mater.* **2015**, *44*, 1044.  
DOI: [10.1007/s11664-014-3617-0](https://doi.org/10.1007/s11664-014-3617-0)
- Kingery, W.D.; Bower, H.K.; Uhlmann, D.R., *Introduction to Ceramics, Wiley, Singapore*, **1991**, 937.
- Buchanan, C., *Ceramic Materials for Electronics: Processing, Properties and Applications*, Marcel Dekker, New York, **1991**.
- Prasad, B. V.; Narsinga Rao, G.; Chen, J. W.; Babu, D. S., *Mater. Research, Bulletin*, **2011**, *46*, 1670.  
DOI: [10.1016/j.materresbull.2011.06.001](https://doi.org/10.1016/j.materresbull.2011.06.001)
- Meena, P.L.; Kumar, R.; Prajapat, C.L.; Sreenivas, K.; Gupta, V., *J. Appl. Phys.* **2009**, *106*, 024105.  
DOI: [10.1063/1.3182722](https://doi.org/10.1063/1.3182722)
- Choudhary, R.J.; Kumar, R.; wasi Khan, M.; Srivastava, J.P.; Arora, S.K.; Shvets, I.V., *Appl. Phys. Lett.* **2005**, *87*, 132104.

DOI: [10.1063/1.2058218](https://doi.org/10.1063/1.2058218)

51. Raymond, O, Font, R., N. Suarez-Almodovar, J. Portelles, and J. M. Siqueiros, *J. Appl. Phys.* **2005**, 97, 084107.

DOI: [10.1063/1.1870099](https://doi.org/10.1063/1.1870099)

## Advanced Materials Letters

Copyright © VBRI Press AB, Sweden

[www.vbripress.com](http://www.vbripress.com)

Publish your article in this journal

Advanced Materials Letters is an official international journal of International Association of Advanced Materials (IAAM, [www.iaamonline.org](http://www.iaamonline.org)) published by VBRI Press AB, Sweden monthly. The journal is intended to provide top-quality peer-review articles in the fascinating field of materials science and technology particularly in the area of structure, synthesis and processing, characterisation, advanced-state properties, and application of materials. All published articles are indexed in various databases and are available download for free. The manuscript management system is completely electronic and has fast and fair peer-review process. The journal includes review article, research article, notes, letter to editor and short communications.

